Reproductive biology of the bathyal asteroid Ctenodiscus crispatus in the northeastern Pacific

Rist, Sinja; Rice, Lauren N.; Plowman, Caitlin Q.; Fountain, C. Tyler; Calhoun, Avery; Ellison, Christina; Young, Craig M.

Published in:
Invertebrate Biology

Link to article, DOI:
10.1111/ivb.12384

Publication date:
2022

Document Version
Publisher's PDF, also known as Version of record

Received: 28 March 2022 | Accepted: 24 August 2022

DOI: 10.1111/ivb.12384

ORIGINAL ARTICLE

Invertebrate Biology WILEY

Reproductive biology of the bathyal asteroid *Ctenodiscus crispatus* in the northeastern Pacific

Sinja Rist[1,2] | Lauren N. Rice[2] | Caitlin Q. Plowman[2] | C. Tyler Fountain[2] | Avery Calhoun[2] | Christina Ellison[2] | Craig M. Young[2]

[1]National Institute of Aquatic Resources, Technical University of Denmark, Kongens Lyngby, Denmark

[2]Oregon Institute of Marine Biology, University of Oregon, Charleston, Oregon, USA

Correspondence
Sinja Rist, National Institute of Aquatic Resources, Technical University of Denmark. Kongens Lyngby, Denmark, and Oregon Institute of Marine Biology, University of Oregon, Charleston, OR USA.
Email: siri@aqua.dtu.dk

Funding information
Oregon legislature; Villum Foundation, Grant/Award Number: 34438; Oregon State University

Abstract

The mud star *Ctenodiscus crispatus* has a broad distribution from Arctic waters into the northern Atlantic and Pacific oceans. Populations in the Atlantic are well studied and show oocyte sizes indicative of continuous gametogenesis with asea-sonal spawning. In contrast, knowledge on the reproductive biology of Pacific populations is lacking. Thus, this study aims to examine the reproduction of *C. crispatus* in the northeastern Pacific. We sampled a population from the Pacific Ocean off Oregon and confirmed the species identity through *16S* and *cytochrome oxidase subunit I* (*COI*) genetic barcoding. The majority of adults were 22–27 mm in size. Oocytes were obtained from dissected gonads soaked in a 1-methyladenine solution and fertilized with spawned sperm. Other individuals were preserved whole in 10% buffered formalin, and oocytes were measured from preserved gonads. Strip-spawned oocytes had a mean diameter of ~485 μm, consistent with Atlantic populations. Sperm had a mean head diameter and flagellum length of 3.1 and 65.9 μm, respectively. The time between first and second cell divisions was ~2 h, but larval cultures failed, and very few embryos developed to blastulae. Both strip-spawned and preserved oocytes had a bimodal size-frequency distribution indicative of semicontinuous gametogenesis. Comparison among individuals showed evidence of asynchrony among the population. This asynchrony and bimodal oocyte distribution may be driven by regular pulses of food, as has been postulated for other populations of this species. The reproductive plasticity seen among populations of this species in different regions could explain how it successfully inhabits such a wide geographic range.

KEYWORDS
circumboreal, DNA barcoding, embryology, gametes, mud star

1 | INTRODUCTION

The mud star *Ctenodiscus crispatus* (BRUZELIUS 1805) is known for its broad longitudinal distribution in boreo-arctic waters (Ekman, 1953). *C. crispatus* has been documented in the Sea of Japan (Kharlamenko et al., 2013), the Beaufort Sea (Rand & Logerwell, 2011), offshore of Newfoundland (Jaramillo, 2001), the Gulf of Maine (Shick, Edwards, & Dearborn, 1981), the west side of Panama (Ekman, 1953; Grainger, 1966), the Barents Sea (Johannesen et al., 2017), the Norwegian coast (Falk-Petersen, 1982), and Cape Hatteras in the western Atlantic (Verrill, 1914). Furthermore, the species can be observed within a depth band ranging 400–2000 m (Carey, 1972; Ringvold et al., 2021; Shick, Edwards, & Dearborn, 1981). Throughout its range, the mud star is known to reach high densities and can dominate the benthic fauna (Piepenburg et al., 1996; Ringvold et al., 2021; Shick, Edwards, & Dearborn, 1981). It acts as a deposit detritivore and is commonly found on soft, muddy sediments (Reed et al., 2021; Shick, Edwards, & Dearborn, 1981) that could provide a stable and organically rich food source (Shick, Taylor, & Lamb, 1981). Individuals construct shallow burrows and feed nonselectively on sediment and various infaunal organisms, including foraminifera, annelids, and pelecypod bivalves (Carey, 1972; Shick, Edwards, & Dearborn, 1981).

Previous research on Atlantic populations of *C. crispatus* has found evidence of continuous reproduction, with indications of aseasonal spawning (Falk-Petersen, 1982; Jaramillo, 2001; Reed et al., 2021). However, Shick, Taylor, and Lamb (1981) also noted that pulses of reproductive output could be tied to phytodetrital falls to the seafloor, which is a conclusion recently supported by Reed et al. (2021). Vitellogenic oocytes for *C. crispatus* are large in diameter, with maximum sizes exceeding 400 μm (Jaramillo, 2001; Reed et al., 2021; Shick, Taylor, & Lamb, 1981). Although the embryology of this species has yet to be observed, lecithotrophic development has been inferred because of the large observed oocyte diameters and the lipid-rich nature of the spawned eggs (Falk-Petersen, 1982). This contrasts with the congener *C. australis*, in which individuals have been found to brood larvae on the aboral side (Rivadeneira et al., 2017).

Despite the broad distribution of *C. crispatus*, relatively few studies have focused on the populations within the Pacific as compared to those in the Atlantic. Several studies have examined the steroid metabolites produced by individuals of *C. crispatus* in the Sea of Japan (Kicha et al., 1994, 2005) and used fatty acid and stable isotope signatures to determine their trophic position within benthic communities (Kharlamenko et al., 2013). Other studies noted the presence and abundance of *C. crispatus* via trawl surveys within the Bering (Rand & Logerwell, 2011) and Beaufort (Lin et al., 2018) seas. However, much of the biology for Pacific-dwelling *C. crispatus* remains unexamined, and the reproductive patterns have yet to be evaluated for any population outside of the Atlantic.

This study seeks to examine the reproductive biology of *C. crispatus* along the Oregon shelf. We present data on adult size, sex ratios, oocyte and sperm size, and the early embryology for individuals collected from this Pacific region. To ensure that our data are comparable with results from Atlantic populations, we also analyzed *16S* and *COI* genes to confirm the identity of this circumboreal species.

2 | METHODS

2.1 | Field collection and animal keeping

Individuals of *C. crispatus* were collected with an Agassiz trawl deployed from the R/V *Oceanus* on August 29, 2021, on the Oregon shelf off Newport, Oregon (average 44.5279°, −124.7576°). The sampling site had a depth of 383 m and was characterized by a soft, muddy bottom with a gentle slope. Immediately after recovery, a random subsample of individuals of *C. crispatus* was collected and transferred to a chilled (7°C) recirculating seawater tank on the ship. After disembarkment 2 days later, the animals were transported to the Oregon Institute of Marine Biology (OIMB) in Charleston, Oregon, where they were placed in a recirculating system of natural seawater chilled to a temperature of 7°C.

2.2 | Genetic barcoding

To confirm species identity genetically, tube feet from three randomly selected individuals were preserved in 95% ethanol for DNA barcoding. DNA was extracted using DNEasy Blood and Tissue Kit (Qiagen™). Two mitochondrial genes, *COI* and *16S* rDNA, were amplified using polymerase chain reaction (PCR). Each PCR was performed in a 20 μl volume with 1 unit per reaction of Go Taq Polymerase (Promega) with supplied buffer, 200 μM dNTPs, and 500 nM of each primer. Universal primers were used for both genes: LCO1490 and HCO2198 for *COI* (Folmer et al., 1994) and 16SARL and 16BRH for *16S* (Palumbi et al., 1991). The PCR cycling parameters were initial denaturation at 95°C for 2 min, 34 cycles of denaturation at 95°C for 40 s, primer annealing at 45°C for *COI* and 50°C for *16S* for 40 s, primer extension at 72°C for 1 min, and a 2 min final extension at 72°C. Successful amplification was verified with gel electrophoresis using 1.0% agarose gel at 150 V for 20 min. PCR products were purified using the Promega SV Wizard Gel and PCR Clean up Kit (Betz & Strader, 2002) and sent to Sequetech in Mountain View, California, for Sanger sequencing in both directions. We used Geneious Prime® 2022.1.1 for all sequence analyses. Sequences were trimmed of primers and low-quality regions, aligned with their complementary strands, proofread, and used to generate consensus sequences, all of which had quality scores >97%. *COI* sequences were translated into amino acids and checked for the presence of stop codons. We used NCBI BLAST to screen for contamination and to verify species identity. Sequences with high similarity to ours were downloaded from GenBank and incorporated into the analysis. The resulting sequences were aligned using the MAFFT plug-in (default parameters), visually inspected for gaps and irregularities, then trimmed to the length of the shortest sequence. The final 465-bp *COI*

alignment was used to build a neighbor-joining tree (default parameters). Percent identity (p distance) was used to evaluate species status with reference to published barcoding values observed within the Asteroidea. Original sequence data were submitted to BOLD (process IDs OSIMB001-22, OSIMB002-22, OSIMB003-22) and GenBank (ON774791-ON774795).

2.3 | Spawning and fertilization

We attempted to induce spawning in the mud stars by injection with 1-methyladenine (1-MA), which has previously been used successfully in this species (Shick, Taylor, & Lamb, 1981). Twenty individuals were chosen randomly, and 0.5 ml of a 0.2 μM 1-MA solution was injected near gonadal tissue by inserting the needle near the mouth. The size of each individual was recorded by measuring the length between the center of the disc and the tip of a ray (*R*, major radius) as well as between the center and the edge of the disc (*r*, minor radius) using a ruler (Lawrence, 2013). Following injection, each mud star was placed into an individual bowl of seawater to monitor for spawning. As spawning was not observed within 2 h, except in one male, a second round of injections with 0.5 ml of a 0.6 μM 1-MA solution was attempted. This, however, did not result in spawning either. Thus, 11 individuals were dissected and the gonads removed for strip-spawning. Dissected gonads were gently macerated and soaked in 0.6 μM 1-MA solution. Oocytes of several females were mixed and fertilized with sperm from the single male that spawned. Fertilization and embryonic development were monitored using a stereomicroscope (Zeiss Stemi 508), and pictures of all stages were taken with a connected camera (Axiocam 208 color). Pictures of fertilization envelopes and sperm were taken on an Olympus BX50 compound microscope with a connected Flea 3 camera by FLIR for quantifying gamete morphometrics. After fertilization was observed, the culture was split into four glass jars with 340 ml of filtered seawater each. They were kept partially submerged in a recirculating seawater system chilled to 7°C and observed every hour for the first 24 h, then once every 12 h thereafter. Malformed embryos were removed from the jars during each observation.

2.4 | Analyses of preserved specimens

All remaining live individuals of *C. crispatus* that had not been used for the spawning and fertilization trials were preserved in 10% buffered formalin. The sizes of all preserved individuals were measured as described above, including specimens of *C. crispatus* from previous cruises on the Oregon shelf and slope in 2016 and 2019; in 2016, six individuals were found in a trawl offshore of Newport, Oregon, from ~900 m depth (average 44.6898°, −124.9940°), and three individuals were collected from 620 m depth near Cape Arago, Oregon, in 2019 (average 43.3434°, −124.7887°).

Specimens from the 2021 cruise were dissected, and gonads were removed for reproductive analysis. Of the 81 preserved specimens from 2021, a random subsample of 20 females was selected to quantify oocyte size distributions. Dissections were made along the ambulacral groove, and paired gonads were excised, rinsed in 70% ethanol, and photographed using a stereomicroscope (Zeiss Stemi 508) with camera attachment (Zeiss Axiocam 208 color). Photographs were analyzed using ImageJ (NIH), and the Feret diameter of 100 random oocytes was measured from each female.

2.5 | Data analysis

ImageJ (NIH) was used for all measurements quantifying the gamete morphometrics of fertilization envelopes, sperm, and oocytes. All graphs and statistical analyses were made in R (version 3.6.3). Before inferential statistics were conducted, normality of the residuals was tested with the Shapiro–Wilk test and homogeneity of variances with the Fligner–Killeen test. The difference between body sizes of females and males was analyzed with a t-test. Oocyte size distributions among the 20 examined females violated data assumptions of normality and as a result were analyzed with a Kruskal–Wallis test. Dunn's multiple comparison test was run post hoc to examine pairwise differences among average oocytes sizes of individual females (supporting information Table S1).

3 | RESULTS

We successfully sequenced *COI* from two of the three sampled individuals and *16S* from all three (Table 1). BLAST and taxon search located 30 *COI* sequences and a single *16S* sequence of *C. crispatus* within GenBank, derived from at least seven locations in the northeastern Pacific, Arctic, and upper northwestern Atlantic oceans (Figure 1). Half of all *COI* sequences were identical. The maximum sequence divergence observed was <1.5% for *COI* and 0.2% for *16S*. Previous barcoding studies suggest that the upper limit of intraspecific divergence in echinoderms for the *COI* gene is 1.6%–3.6% (Collin et al., 2020; Corstorphine, 2010; Laakmann et al., 2017; Ward et al., 2008), confirming that all sequences originate from members of the same species.

Beyond the species level, there are no close relatives of *C. crispatus* in GenBank. The next 20 closest matches converge at 82% similarity and represent a variety of orders and superorders in the infraclass Neoasteroidea.

Whereas *COI* confirms the presence of *C. crispatus* in part of its reported range, as far as we know, no barcodes are available for individuals from the northeastern Atlantic, northwestern Pacific, or those farther south than the upper northwestern Atlantic; however, five GenBank sequences were not associated with any collection location and could be from one of these. Further barcoding efforts are needed to elucidate the biogeography of this taxon and ensure reproductive characters are comparable.The measurements of adult sizes revealed a consistent *R* (major radius) to *r* (minor radius) ratio of 2.2 ± 0.2 across all specimens. Therefore, the major radius was used to report

Specimen	GenBank *16S*	GenBank *COI*	BOLD process ID
Ctendodiscus crispatus #23	ON774792	N/A	OSIMB001–22
Ctendodiscus crispatus #24	ON774793	ON774795	OSIMB002–22
Ctendodiscus crispatus #25	ON774791	ON774794	OSIMB003–22

Abbreviation: *COI*, *cytochrome oxidase subunit I*.

TABLE 1 GenBank accession numbers and BOLD IDs for sequenced specimens

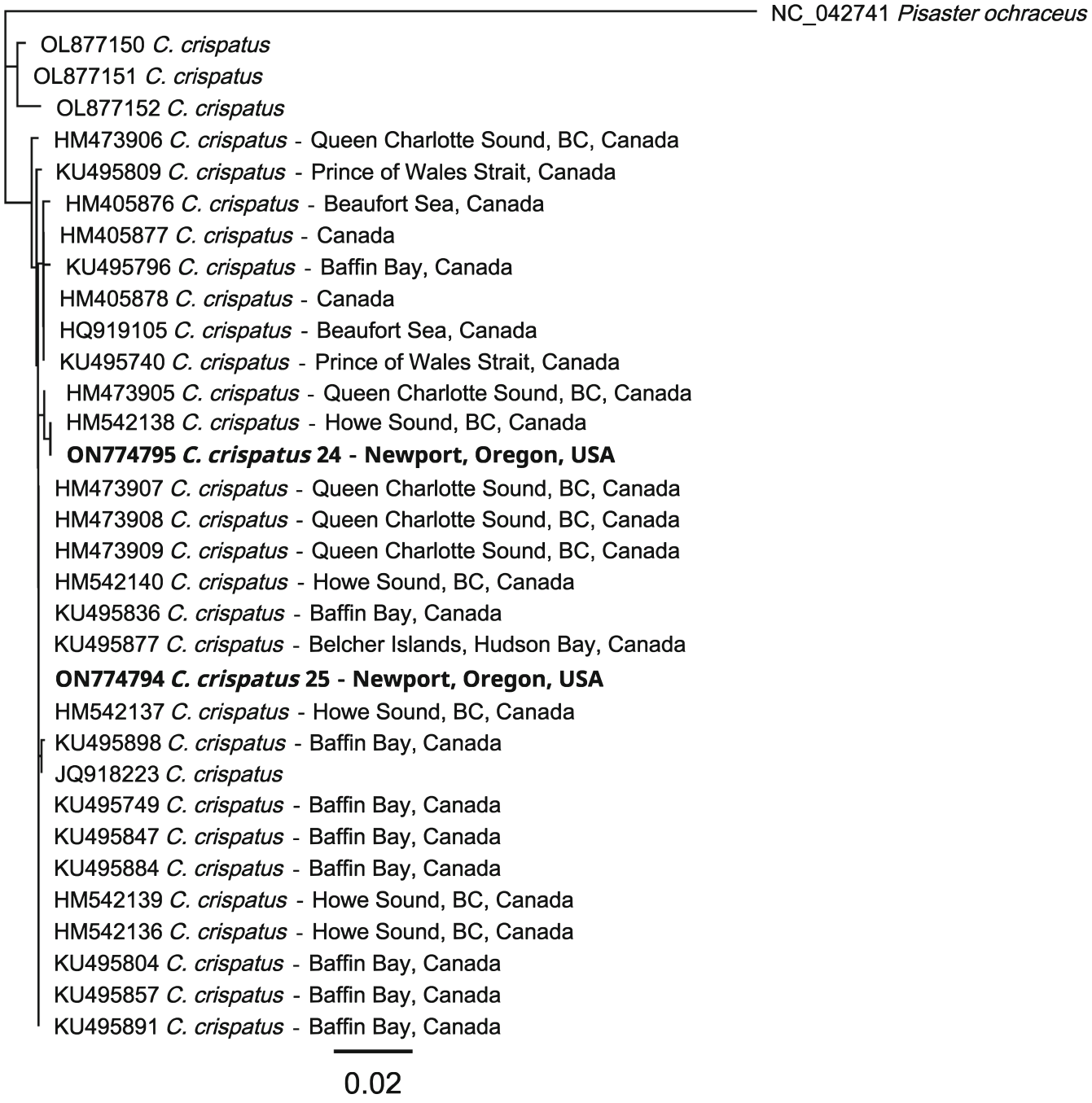

FIGURE 1 *COI* neighbor-joining tree (Tamura Nei) of sequences from 32 individuals of *Ctenodiscus crispatus*; the tree is rooted by the closest outgroup sequence in GenBank. Scale bar represents 2% sequence divergence. Sequences original to this study are bolded; all others were mined from GenBank. Collection locations indicated, if available

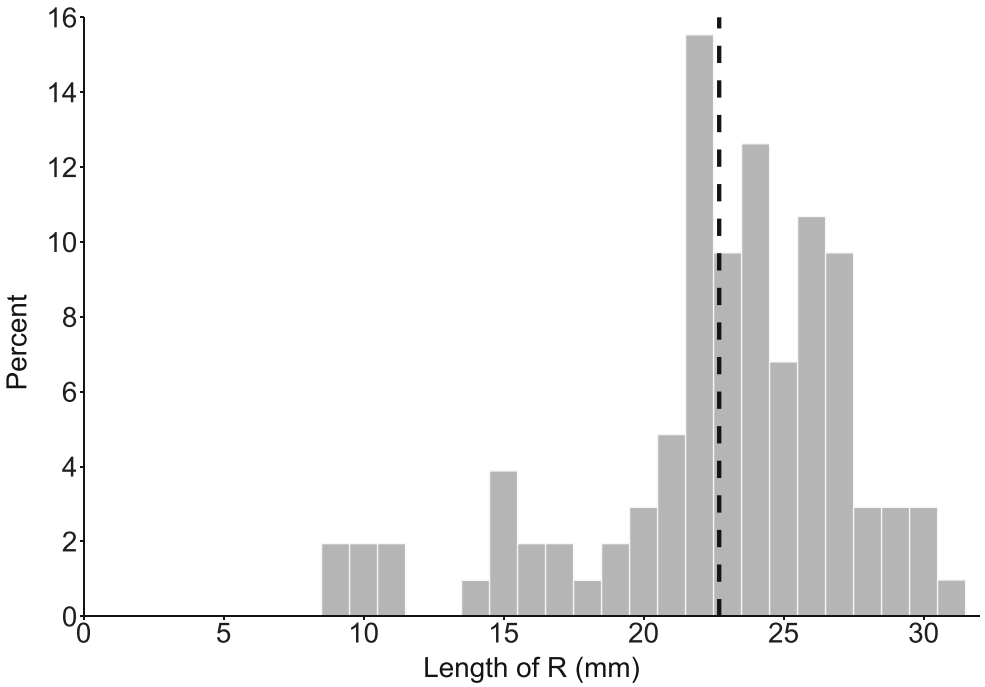

FIGURE 2 Size-frequency distribution of adults of *Ctenodiscus crispatus* on the Oregon shelf. R is the major radius. Samples were collected between 383 and 900 m during three separate research cruises in 2016 ($n = 6$ individuals), 2019 ($n = 3$), and 2021 ($n = 94$). Bin width is 1 mm. The dashed line indicates the mean size (22.7 mm) across all individuals

adult size. The size of individuals collected in 2021 ranged 9–31 mm, with 60% having a length of 22–27 mm (Figure 2). The mean length was 23.4 ± 4.4 mm, with males being on average 1.2 mm larger than females. This difference was, however, not significant (two-sample t-test, $t = -1.7$, $df = 37.4$, $p = 0.09$). Dissected individuals were gonochoristic with an equal sex ratio of females to males. The smallest individual with mature gonads had a length of 20 mm. The six individuals from collections in 2016 had a length between 14 and 21 mm with a mean of 15.8 ± 3 mm, and the three individuals from 2019 were 16, 17, and 18 mm in length.

In living specimens of *C. crispatus*, females were clearly recognizable by the orange color of the gonads that were visible through the oral surface (Figure 3C). Paired gonads are located internally between the arms and are connected by gonoducts to two gonopores on the oral surface that lie between each pair of arms. Gonopores were clearly visible in the spawning male (Figure 3A). We did not observe any response to injections with 1-MA, except in one male individual. When dissecting out gonads, we found a few females whose oocytes had a yellow color instead of the more common bright orange. These consistently failed to fertilize, in contrast to orange oocytes. The diameter of oocytes acquired through strip-spawning varied between 299.8 and 618 μm, with a mean size of 485.4 ± 62.7 μm. The size-frequency distribution followed a bimodal pattern (Figure 4A). The majority (72.5%) of oocytes were in the bigger size range, >460 μm, whereas 27.5% were in the smaller range.

Additional morphometric data were gathered while analyzing sperm and fertilization envelopes. Sperm, collected from the spawning male, had a standard morphology of a small head with a single flagellum (Figure 3D). The average diameter of sperm heads was 3.1 ± 0.4 μm, with minimum and maximum diameters of 2.6 and 4.3 μm, respectively. The length of the sperm tails ranged 42.6–79.5 μm, with an average length of 65.9 ± 9 μm. We observed several aggregates of three to six sperm heads occurring among the individual sperm. Successful fertilization resulted in the formation of a visible fertilization envelope (Figure 3E). The diameter of this envelope varied between 415.1 and 671.1 μm. However, 80% fell into a narrow range of 529–598.9 μm, and the mean size was 564.3 ± 31.6 μm (Figure 4B).

The first cell division was observed 8 h postfertilization (Figure 3F), and the time between first and second cell divisions was about 2 h, after which subsequent cell divisions occurred in intervals of 1–2 h (Table 2). Cell divisions were radial holoblastic. Cultured embryos started to die off ~35 h postfertilization, and only a few embryos developed to blastulae. Eggs and embryos were positively buoyant in seawater, whereas blastulae began sinking.

Oocyte sizes were also measured in 20 preserved females from the 2021 collection that had not been used for spawning. The diameter of oocytes measured through the membrane of preserved and dissected gonads ranged 60–623 μm, with a mean size of 292.3 ± 122.2 μm. Each female had oocytes present in a broad range of sizes, and the population average size-frequency distribution had a clear bimodal pattern around the mean (Figure 5A). Individuals also exhibited a similar pattern of bimodality in oocyte sizes (Figure 5B), but distributions varied significantly (Kruskal–Wallis, $\chi^2 = 174.88$, $df = 19$, $p < 0.05$). Out of 190 pairwise comparisons, 47 were significantly different (Table S1). The largest individuals were more different from others than smaller stars. In the case of Individuals 13, 18, 19, and 20, the oocyte size distribution was shifted toward larger oocytes, whereas Individual 17 had a bigger fraction of small oocytes.

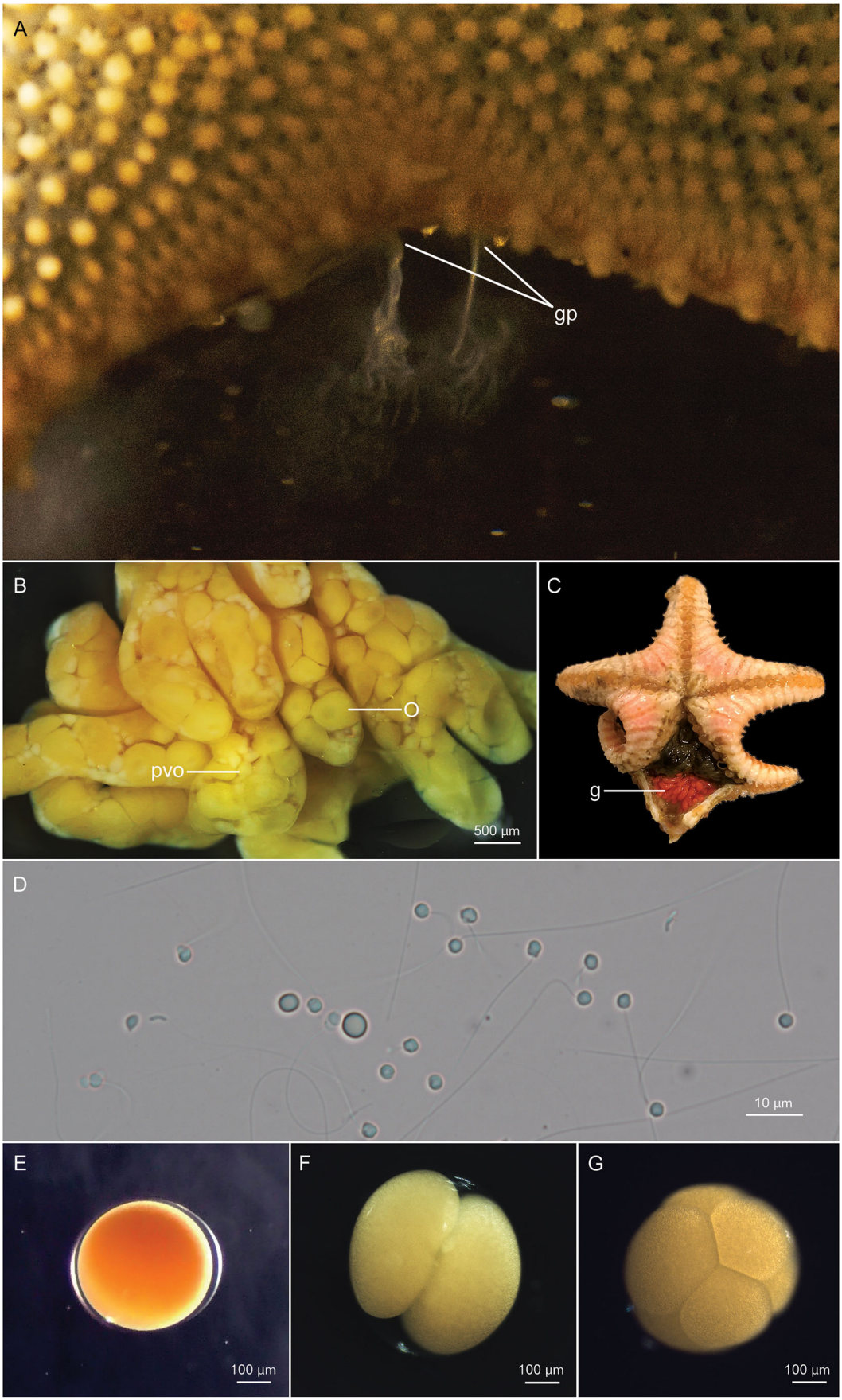

FIGURE 3 Legend on next page.

FIGURE 3 (A) Spawning male of *Ctenodiscus crispatus*, with paired gonopores (gp). (B) Dissected gonads of a female of *C. crispatus*, showing both previtellogenic oocytes (pvo) and mature oocytes (O). (C) Oral side of a female, with gonads (g) in bright orange located between the arms. (D) Spermatozoa. (E) Oocyte with a fertilization envelope. (F) 2-cell stage embryo (8 h postfertilization). (G) 8-cell stage embryo (11 h postfertilization)

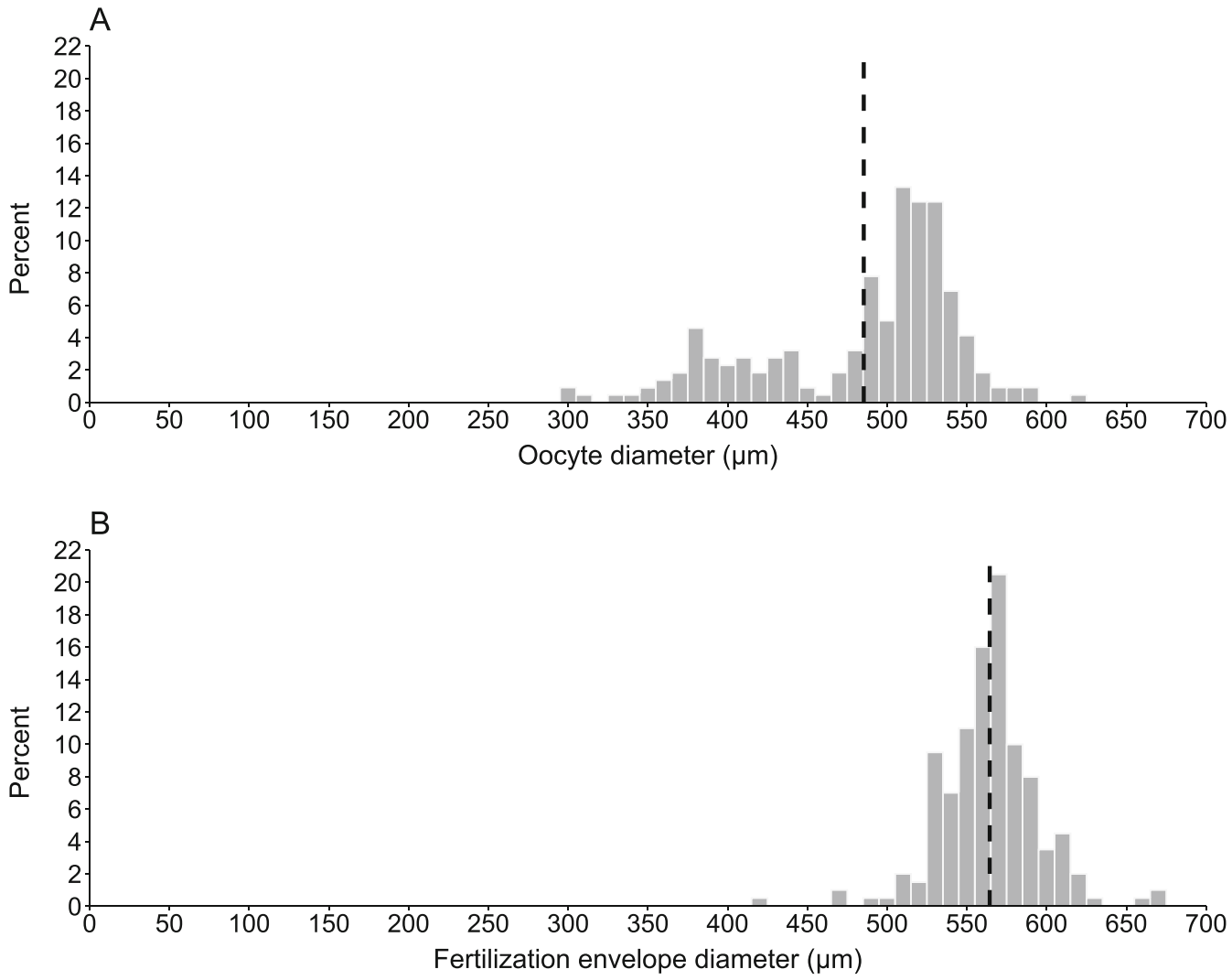

FIGURE 4 (A) Size-frequency distribution of strip-spawned oocytes ($n = 218$) from females of *Ctenodiscus crispatus*. Dashed line indicates the mean size of oocytes (485.36 μm). (B) Frequency of fertilization envelope diameters ($n = 200$). Dashed line indicates mean diameter of fertilization envelopes (564.34 μm). Bin width in both panels is 10 μm

TABLE 2 Timing of early cell divisions in embryos of *Ctenodiscus crispatus* reared in filtered seawater at 7°C

Event	Hours postfertilization
Fertilization	0
First cell division	8
Second cell division	10
Third cell division	11
Fourth cell division	13
Fifth cell division	15

4 | DISCUSSION

C. crispatus has been described to be widely distributed among its circumboreal range and abundant or even dominating among soft-bottom marine communities (Jaramillo, 2001; Reed et al., 2021; Shick, Edwards, & Dearborn, 1981; Tranang, 2017). Between 2016 and 2021, 42 trawls were conducted along the Oregon shelf over a variety of substratum types including sand, mud, rock, and gravel, but the single reported trawl in 2021 contained the only large sampling of this species (Young, unpublished data). This alludes to a rather patchy

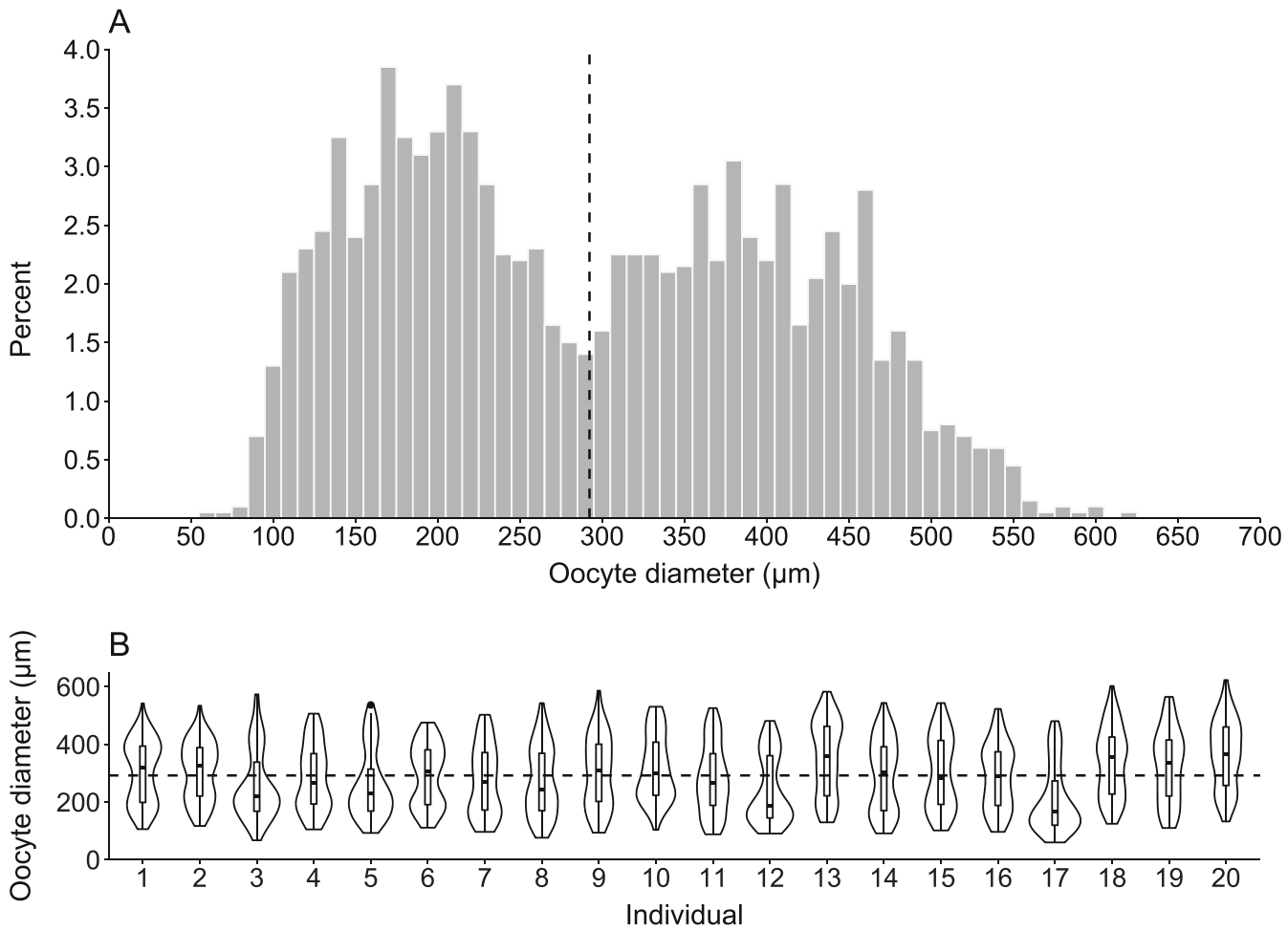

FIGURE 5 (A) Population average oocyte size-frequency distribution for 20 females ($n = 2000$ oocytes) of *Ctenodiscus crispatus* from the research cruise in 2021. Oocytes were measured through the outer membrane of preserved and dissected gonads. Bin width is 10 μm. (B) Individual oocyte size-frequency distributions for the same 20 females. Individuals are ordered in increasing size from 20 (1) to 27 mm (20). In both graphs, the dashed line indicates the mean size across all oocytes (292.32 μm)

distribution in this region, a pattern which has also been observed for this species in the Barents Sea (Solan et al., 2020). However, a systematic study is needed to determine the distribution and abundance of *C. crispatus* on the Oregon shelf and slope and indeed throughout the full reported range of this species.

The observed size range of *C. crispatus* collected on the Oregon shelf (9–31 mm) falls within the reported range of individuals sampled from the Barents Sea (~3–31 mm, Reed et al., 2021) and the Gulf of Maine (~17–36 mm, Shick, Taylor, & Lamb, 1981). A bimodal size distribution of *C. crispatus* was observed in Balsfjord, Svalbard (Tranang, 2017); however, our data show a left-skewed trend toward larger individuals. It has been hypothesized that juveniles grow rapidly to adulthood, after which growth and mortality rates are low, potentially explaining the observation of larger individuals (Tranang, 2017). Additionally, the minimum observed size of adults in this study with mature gonads (20 mm) was slightly larger than what has been reported from the Barents Sea (13.7 mm, Reed et al., 2021) and Gulf of Maine (~17 mm, Shick, Taylor, & Lamb, 1981) but smaller than in Newfoundland (22 mm, Jaramillo, 2001). The variation in reported minimum reproductive sizes between locations could indicate regional differences in environmental factors such as food availability. For example, if a region has more frequent pulses of detrital flux to the benthos, individuals of *C. crispatus* might be able to begin gametogenesis earlier than in areas with more periodic nutrient subsidies.

The size range of oocytes obtained by strip-spawning (299.8–618 μm) overlaps with previously reported values (Falk-Petersen, 1982), although larger oocytes ranging 260–983 μm were recorded off Newfoundland (Jaramillo, 2001). Although detailed morphological descriptions of sperm exist for *C. crispatus* (Summers et al., 1975), to our knowledge, this is the first study quantifying sperm size. Observed sperm displayed common morphological characteristics seen in asteroids with a spheroidal head and a single long flagellum. Our sperm head diameters were larger than those reported for other echinoderms (Chia et al., 1975); however, those measurements were mostly made on preserved sperm, and preservation often causes shrinkage.

Observations of large yolk-rich oocytes during strip-spawning and embryological investigation support previous suggestions that

lecithotrophic larval development is present in *C. crispatus* (Falk-Petersen, 1982). Although our culture failed to grow past the blastula stage (35 h postfertilization), insight was gained into rearing larvae of *C. crispatus*. Collected individuals of *C. crispatus* deteriorated quickly after being placed in captivity and did not respond to 1-MA despite previous reports that this would induce spawning (Shick, Taylor, & Lamb, 1981); as a result, strip-spawned oocytes were used and were likely of lower quality. Similarly, attempts by Jaramillo (2001) to induce spawning with NaCl failed. Of the strip-spawned oocytes, only large, bright orange, and positively buoyant oocytes were kept for our study. Our cultures were reared without mixing; however, oxygenation of cultures via drip line or stir rack is likely to produce better results. Successful fertilization was visible by the formation of a fertilization envelope, and fertilized oocytes displayed a narrow size range around a mean of 564.3 μm, indicating that only the larger fraction of strip-spawned oocytes was fertilized. All cell divisions after the first occurred in regular intervals of 1–2 h. We were not able to find timelines of early cell divisions for closely related species. However, another local subtidal asteroid, *Crossaster papposus*, which is larger in size, also develops in ∼2 h from two to four cells (Strathmann et al., 2002).

The measurements of oocytes in the gonads of preserved and dissected females revealed a wider bimodal size range (60–623 μm), with the majority being substantially smaller than strip-spawned oocytes. Preservation in formalin is known to result in tissue shrinkage, and the membrane of the gonad keeps oocytes compressed, so these values are not directly comparable with those of spawned eggs. When comparing our oocyte size range with literature values of preserved gonads, we saw a clear overlap among samples collected from the Gulf of Maine (15–400 μm, Shick, Taylor, & Lamb, 1981), offshore Newfoundland (50–550 μm, Jaramillo, 2001), and the Barents Sea (24–500 μm, Reed et al., 2021); however, our maximum size is larger than those previously reported from histological sections.

The wide size range of oocytes is indicative of continuous gametogenesis, and the presence of mature oocytes throughout the year has been reported for populations in Newfoundland (Jaramillo, 2001), the Gulf of Maine (Shick, Taylor, & Lamb, 1981), and Ramfjorden, Norway (Falk-Petersen, 1982). Our size-frequency distribution of oocytes displayed a clear bimodality, both for the population as a whole and within most individuals. Significant differences in oocyte size distributions between several individuals suggest that gametogenesis can be asynchronous at the individual level, resulting in semicontinuous reproductive output of females at the population level. Because larger individuals exhibited a more skewed oocyte size distribution, we hypothesize that these were either close to spawning (e.g., Individuals 18 and 20) or had recently spawned (e.g., Individual 17). Larger individuals may be able to acquire more food and/or allocate more nutrients to reproduction. In order to test this further, a full reproductive study with regular sampling throughout the year is recommended. Such clear bimodality of oocyte size has not been described for other populations of *C. crispatus*, although four distinct modes interpreted as four separate cohorts of mature oocytes were present throughout the year within the Gulf of Maine population (Shick, Taylor, & Lamb, 1981). Midwinter was postulated to be the season of primary oogenesis, with spawning taking place in April–May and October–November, as indicated by the disappearance of large oocytes during these times (Shick, Taylor, & Lamb, 1981). Seasonal patterns were also observed in Ramfjorden, Norway, with the number of mature oocytes peaking September through January, and spawning was easiest to induce in autumn and in May (Falk-Petersen, 1982). In contrast, no seasonal variation in oocyte size has been reported in Newfoundland (Jaramillo, 2001). Oocyte size distributions may be influenced by the potential influx of seasonal phytodetritus (Reed et al., 2021); aseasonality in reproduction has been attributed to the stable and organically complex nutrition provided by the sediment (Shick, Edwards, & Dearborn, 1981).

It is difficult to distinguish whether differences between our results and previous studies are merely relics of disparate methodologies or are evidence to suggest that *C. crispatus* exhibits regional differences in body and oocyte size. From genetic analyses, our results corroborate the idea that *C. crispatus* is a circumboreal species, and quantitative investigation examining adult sizes, gamete sizes, and reproductive patterns suggest that individuals from the eastern Pacific are comparable with northern Atlantic and subarctic populations. A comparative approach investigating variability in reproduction and embryological development across the species range will allow future studies to examine how seasonal and regional differences in environmental conditions, in addition to nutrient availability, shape the reproductive capacity of *C. crispatus*.

To the best of our knowledge, this is the first report showing a difference in reproductive strategy between starfish occurring in two different ocean basins. A search of the literature (Clark & Downey, 1992; Mortensen, 1927) reveals seven asteroid species with similar patterns of distribution. Three of these are brooders and the remaining ones have large eggs that produce (or likely produce) lecithotrophic larvae. However, before the present study, the reproduction of only two circumboreal species, *Solaster endeca* and *C. papposus*, has been examined in both the Atlantic and Pacific oceans. Gemmill (1912, 1920) described the embryology of both species in detail and noted that the spawning was annual, peaking in March and April. Both of these species have the same periodicity in the northeastern Pacific (anecdotal reports in Strathmann, 1987). It is interesting that these shallow subtidal species have the same annual peak as the majority of other echinoderm species at similar depths and latitudes in the Pacific (Strathmann, 1987), many of which use either bright sunlight or lunar periodicity as a spawning cue (Pearse et al., 1988). *C. crispatus* occurs at a depth where such cues are not available and has evolved different reproductive periods in different parts of its range. It would be instructive to investigate the cues and environmental factors that underlie this difference in gametogenic cycles between oceans.

ACKNOWLEDGMENTS

We express gratitude to A. Germán-Castañeda, S. Joy, and N. Nakata (OIMB Fall 2021 Marine Molecular Biology class) for their help with

DNA extraction and PCR. The Captain and crew of the R/V *Oceanus* provided expert support in collecting samples from deep water. Ship time on R/V *Oceanus* was funded by a grant to CMY from the Oregon legislature, administered by Oregon State University. We would also like to thank the Villum Foundation for financial support to SR through the project PELAGIC (project no. 34438).

CONFLICT OF INTEREST

The authors declare no conflict of interest.

ORCID

Sinja Rist https://orcid.org/0000-0003-3002-0793

REFERENCES

Betz, N., & Strader, T. (2002). Clean-up with Wizard SV for gel and PCR. *Promega Notes*, *82*, 1–5.

Carey, A. G. (1972). Food sources of sublittoral, bathyal and abyssal asteroids in the northeast Pacific Ocean. *Ophelia*, *10*(1), 35–47. https://doi.org/10.1080/00785326.1972.10430100

Chia, F., Atwood, D., & Crawford, B. (1975). Comparative Morphology of Echinoderm Sperm and Possible Phylogenetic Implications. *American Zoologist*, *15*(3), 553–565.

Clark, A. M., & Downey, M. E. (1992). Starfishes of the Atlantic. In *Chapman and Hall Identification Guides*, *3*. Hall.

Collin, R., Venera-Pontón, D. E., Driskell, A. C., Macdonald, K. S., & Boyle, M. J. (2020). How I wonder what you are: Can DNA barcoding identify the larval asteroids of Panama? *Invertebrate Biology*, *139*(4), e12303. https://doi.org/10.1111/ivb.12303

Corstorphine, E. A. (2010). *DNA barcoding of echinoderms: Species diversity and patterns of molecular evolution* [Doctoral dissertation, University of Guelph]. Library and Archives Canada. https://atrium.lib.uoguelph.ca/xmlui/bitstream/handle/10214/20441/Corstorphine_ErinA_MSc.pdf?sequence=1

Ekman, S. (1953). *Zoogeography of the sea*. Sidgwick and Jackson Limited.

Falk-Petersen, I.-B. (1982). Reproductive and biochemical studies of the asteroid *Ctenodiscus crispatus* (Retzius). *Sarsia*, *67*(2), 123–130. https://doi.org/10.1080/00364827.1982.10420538

Folmer, O., Black, M., Hoeh, W., Lutz, R., & Vrijenhoek, R. (1994). DNA primers for amplification of mitochondrial cytochrome c oxidase subunit I from diverse metazoan invertebrates. *Molecular Marine Biology and Biotechnology*, *3*(5), 294–299.

Gemmill, J. F. (1912). The development of the starfish *Solaster endeca* Forbes. *Transactions of the Zoological Society of London*, *20*, 1–58.

Gemmill, J. F. (1920). The development of the starfish *Crossaster papposus*, Muller and Troschel. *Quarterly Journal of Microscopical Science*, *64*, 155–190.

Grainger, E. H. (1966). Sea stars (Echinodermata: Asteroidea) of Arctic North America. *Bulletin of the Fisheries Research Board Canada*, *152*, 1–70.

Jaramillo, J. R. (2001). *The effects of a Seasonal pulse of sinking phytodetritus on the reproduction of the two benthic deposit-feeding species, Yoldia hyperborea and Ctenodiscus crispatus* [Doctoral dissertation. Memorial University of Newfoundland]. https://research.library.mun.ca/1476/

Johannesen, E., Jørgensen, L. L., Fossheim, M., Primicerio, R., Greenacre, M., Ljubin, P. A., Dolgov, A. V., Ingvaldsen, R. B., Anisimova, N. A., & Manushin, I. E. (2017). Large-scale patterns in community structure of benthos and fish in the Barents Sea. *Polar Biology*, *40*(2), 237–246. https://doi.org/10.1007/s00300-016-1946-6

Kharlamenko, V. I., Brandt, A., Kiyashko, S. I., & Würzberg, L. (2013). Trophic relationship of benthic invertebrate fauna from the continental slope of the Sea of Japan. *Deep Sea Research Part II: Topical Studies in Oceanography*, *86–87*, 34–42. https://doi.org/10.1016/j.dsr2.2012.08.007

Kicha, A. A., Ivanchina, N. V., Kalinovsky, A. I., Dmitrenok, P. S., & Stonik, V. A. (2005). Structures of new polar steroids from the Far-Eastern starfish *Ctenodiscus crispatus*. *Russian Chemical Bulletin*, *54*(5), 1266–1271. https://doi.org/10.1007/s11172-005-0392-3

Kicha, A. A., Kalinovskii, A. I., Ivanchina, N. I., El'kin, Y. N., & Stonik, V. A. (1994). Polyhydroxysteroids from the Far-Eastern starfish *Ctenodiscus crispatus*. *Russian Chemical Bulletin*, *43*(10), 1726–1730. https://doi.org/10.1007/BF00703498

Laakmann, S., Boos, K., Knebelsberger, T., Raupach, M. J., & Neumann, H. (2017). Species identification of echinoderms from the North Sea by combining morphology and molecular data. *Helgoland Marine Research*, *70*(1), 1–18. https://doi.org/10.1186/s10152-016-0468-5

Lawrence, J. M. (2013). *Starfish: Biology and ecology of the Asteroidea*. The John Hopkins University Press.

Lin, H., Liu, K., Wang, J., Huang, Y., Li, Z., Lin, J., He, X., Zhang, S., Mou, J., Wang, Y., & Xing, B. (2018). Spatial pattern of macrobenthic communities along a shelf-slope-basin transect across the Bering Sea. *Acta Oceanologica Sinica*, *37*(6), 72–81. https://doi.org/10.1007/s13131-018-1192-6

Mortensen, T. (1927). *Handbook of the echinoderms of the British Isles*. Oxford Univeristy Press.

Palumbi, S., Martin, A., Romano, S., McMillan, W. O., Stice, L., & Grabowski, G. (1991). *The simple fools guide to PCR, Version 2.0*. University of Hawaii Press.

Pearse, J. S., McClary, D. J., Sewell, M. A., Austin, W. C., Perez-Ruzafa, A., & Byrne, M. (1988). Simultaneous spawning of six species of echinoderms in Barkley Sound, British Columbia. *International Journal of Invertebrate Reproduction and Development*, *14*(2–3), 279–288.

Piepenburg, D., von Dorrien, C. F., Schmid, M. K., Chernova, N. V., Neyelov, A. V., Gutt, J., Rachor, E., & Saldanha, L. (1996). Megabenthic communities in the waters around Svalbard. *Polar Biology*, *16*, 431–446.

Rand, K. M., & Logerwell, E. A. (2011). The first demersal trawl survey of benthic fish and invertebrates in the Beaufort Sea since the late 1970s. *Polar Biology*, *34*(4), 475–488. https://doi.org/10.1007/s00300-010-0900-2

Reed, A. J., Godbold, J. A., Solan, M., & Grange, L. J. (2021). Reproductive traits and population dynamics of benthic invertebrates indicate episodic recruitment patterns across an Arctic polar front. *Ecology and Evolution*, *11*(11), 6900–6912. https://doi.org/10.1002/ece3.7539

Ringvold, H., Guðmundsson, G., & Andersen, T. (2021). Starfish (Asteroidea, Echinodermata) from Iceland; spatial distribution and abundance. *Deep Sea Research Part I: Oceanographic Research Papers*, *176*, 103605. https://doi.org/10.1016/j.dsr.2021.103605

Rivadeneira, P. R., Brogger, M. I., & Penchaszadeh, P. E. (2017). Aboral brooding in the deep water sea star *Ctenodiscus australis* Lütken, 1871 (Asteroidea) from the Southwestern Atlantic. *Deep Sea Research Part I: Oceanographic Research Papers*, *123*, 105–109. https://doi.org/10.1016/j.dsr.2017.03.011

Shick, J. M., Edwards, K., & Dearborn, J. (1981). Physiological ecology of the deposit-feeding sea star *Ctenodiscus crispatus*: Ciliated surfaces and animal-sediment interactions. *Marine Ecology Progress Series*, *5*(2), 165–184. https://doi.org/10.3354/meps005165

Shick, J. M., Taylor, W. F., & Lamb, A. N. (1981). Reproduction and genetic variation in the deposit-feeding sea star *Ctenodiscus crispatus*. *Marine Biology*, *63*(1), 51–66. https://doi.org/10.1007/BF00394662

Solan, M., Ward, E. R., Wood, C. L., Reed, A. J., Grange, L. J., & Godbold, J. A. (2020). Climate-driven benthic invertebrate acitivity and biogeochemical functioning across the Barents Sea polar front.

Philosophical Transactions of the Royal Society A, *378*, 201903. https://doi.org/10.1098/rsta.2019.0365

Strathmann, M. F. (1987). *Reproduction and development of marine invertebrates of the northern Pacific coast: Data and methods for the study of eggs, embryos, and larvae*. University of Washington Press. http://www.jstor.org/stable/j.ctvcwnh8b

Strathmann, R. R., Staver, J. M., & Hoffman, J. R. (2002). Risk and the evolution of cell-cycle durations of embryos. *Evolution*, *56*(4), 708–720. https://doi.org/10.1111/j.0014-3820.2002.tb01382.x

Summers, R. G., Hylander, B. L., Colwin, L. H., & Colwin, A. L. (1975). The Functional anatomy of the echinoderm spermatozoon and its interaction with the egg at fertilization. *American Zoologist*, *15*(3), 523–551. https://doi.org/10.1093/icb/15.3.523

Tranang, C. A. (2017). *Epibenthic fauna in Balsfjord* [Master's thesis. The Arctic University of Norway]. https://hdl.handle.net/10037/11341

Verrill, A. E. (1914). *Monograph of the shallow-water starfishes of the North Pacific coast from the Arctic Ocean to California*. Smithsonian Institution. https://doi.org/10.1126/science.40.1032.523

Ward, R. D., Holmes, B. H., & O'Hara, T. D. (2008). DNA barcoding discriminates echinoderm species. *Molecular Ecology Resources*, *8*(6), 1202–1211. https://doi.org/10.1111/j.1755-0998.2008.02332.x

SUPPORTING INFORMATION

Additional supporting information can be found online in the Supporting Information section at the end of this article.

How to cite this article: Rist, S., Rice, L. N., Plowman, C. Q., Fountain, C. T., Calhoun, A., Ellison, C., & Young, C. M. (2022). Reproductive biology of the bathyal asteroid *Ctenodiscus crispatus* in the northeastern Pacific. *Invertebrate Biology*, *141*(4), e12384. https://doi.org/10.1111/ivb.12384